

GRB 081203A: *Swift* UVOT captures the earliest ultraviolet spectrum of a gamma-ray burst

N. P. M. Kuin,^{1*} W. Landsman,² M. J. Page,¹ P. Schady,¹ M. Still,¹ A. A. Breeveld,¹ M. De Pasquale,¹ P. W. A. Roming,³ P. J. Brown,³ M. Carter,¹ C. James,¹ P. A. Curran,¹ A. Cucchiara,³ C. Gronwall,³ S. T. Holland,² E. A. Hoversten,³ S. Hunsberger,³ T. Kennedy,¹ S. Koch,³ H. Lamoureux,¹ F. E. Marshall,² S. R. Oates,¹ A. Parsons,² D. M. Palmer⁴ and P. J. Smith¹

¹Mullard Space Science Laboratory/UCL, Holmbury St Mary, Dorking, Surrey RH5 6NT

²NASA/Goddard Space Flight Center, Greenbelt, MD 20771, USA

³Department of Astronomy & Astrophysics, Penn State University, 525 Davey Laboratory, University Park, PA 16802, USA

⁴Los Alamos National Laboratory, PO Box 1663, Los Alamos, NM 87545, USA

Accepted 2008 January 27. Received 2009 January 27; in original form 2008 December 15

ABSTRACT

We present the earliest ultraviolet (UV) spectrum of a gamma-ray burst (GRB) as observed with the *Swift* Ultra-Violet/Optical Telescope (UVOT). The GRB 081203A spectrum was observed for 50 s with the UV-grism starting 251 s after the *Swift*-Burst-Alert-Telescope (BAT) trigger. During this time, the GRB was ≈ 13.4 mag (u filter) and was still rising to its peak optical brightness. In the UV-grism spectrum, we find a damped Ly α line, Ly β and the Lyman continuum break at a redshift $z = 2.05 \pm 0.01$. A model fit to the Lyman absorption implies a gas column density of $\log N_{\text{H I}} = 22.0 \pm 0.1 \text{ cm}^{-2}$, which is typical of GRB host galaxies with damped Ly α absorbers. This observation of GRB 081203A demonstrates that for brighter GRBs ($v \approx 14$ mag) with moderate redshift ($0.5 < z < 3.5$) the UVOT is able to provide redshifts, and probe for damped Ly α absorbers within 4–6 min from the time of the *Swift*-BAT trigger.

Key words: instrumentation: spectrographs – gamma-rays: bursts.

1 INTRODUCTION

Gamma-ray bursts (GRBs) are the most luminous cosmic explosions known, and their afterglows extend throughout the electromagnetic spectrum, from X-ray to radio wavelengths. Spectra of GRB afterglows in the ultraviolet (UV) to optical wavelength range are particularly important for the study of GRBs, because the spectral positions of absorption lines from the surrounding environment provide the redshifts and, hence, the distances and luminosities of GRBs. Under exceptionally favourable conditions, prompt, very near-UV GRB spectra have been obtained from the ground (i.e. Very Large Telescope UVES, which, in principle, is sensitive to wavelengths longwards of 3000 Å, observed a GRB in ≈ 10 min). However, such observations are rare due to atmospheric limitations, time of occurrence and the source position in the sky. Shorter wavelength UV GRB spectra have so far only been taken with the *Hubble Space Telescope*/STIS (Smette et al. 2001), at least 3 days after the GRB trigger. In this Letter, we present the first prompt UV

spectrum of a GRB. The spectrum was obtained with the UV-grism of the *Swift* Ultra-Violet/Optical Telescope (UVOT; Roming et al. 2005).

Since the launch of the *Swift* satellite (Gehrels et al. 2004) in 2004, the UVOT has been making prompt photometric observations of GRBs in the optical and UV simultaneously with the X-ray and gamma-ray observations taken by the X-Ray Telescope (XRT; Burrows et al. 2005) and the Burst Alert Telescope (BAT; Barthelmy et al. 2005), respectively. The UVOT photometric system (Poole et al. 2008) provides photometry in three UV and three optical bands and in one *white* filter which is sensitive over the range of 1700–8000 Å.

Two grisms are also included in the UVOT filter wheel to enable spectra of GRBs to be obtained. Until recently they have not been used in the GRB observing sequence because early in the mission the data indicated that most GRB afterglows were too faint for grism observations, even at early times (Roming et al. 2006). However, after four years of *Swift* observations, our GRB sample is large enough that we can meaningfully reassess the frequency of GRB afterglows which are bright enough for grism spectroscopy, and ascertain the optimum timing for their inclusion in the automated

*E-mail: npmk@mssl.ucl.ac.uk

observing sequence. The catalogue of GRB afterglows observed with the UVOT in the first two and a half years (Roming et al. 2009) shows that UVOT observes ≈ 90 each year, of which ≈ 25 are detected by UVOT in at least one exposure. In its first four years of operation, *Swift* observed five GRBs (GRB 050525A, GRB 050922C, GRB 061007, GRB 080319B and GRB 080810) brighter than the 14th magnitude in *v*. It is GRBs like these that should provide good spectra through the UVOT grisms.

The UV-grism was introduced into the automated UVOT GRB response on 2008 October 7. In this latest sequence, the grism spectrum is 50 s long, preceded by an initial 150 s *white*-filter finding chart and followed by a second finding chart in the *u* filter. With a median *Swift* slew time of 86 s (Roming et al. 2009), the grism observation typically begins 225–275 s after the burst trigger and covers the wavelength range from ≈ 1700 to 5800 \AA . The onboard software autonomously replaces the grism exposure with a *u*-filter exposure for bursts which are faint in the BAT, and therefore unlikely to be viable grism targets.

In the following sections, we present the first grism image of a GRB taken with the UVOT UV-grism, the resulting spectrum of GRB 081203A and its corresponding analysis.

2 OBSERVATIONS AND DATA REDUCTION

The BAT instrument triggered on GRB 081203A at $T = 2008-12-03$ at 13:57:11 UT (Parsons et al. 2008). The mask-weighted light curve showed two overlapping peaks: the first starts at $T - 69$ s and peaks at $T + 10$ s, the second peaks at $T + 32$ s and ends at $T + 405$ s. UVOT started settled observations of GRB 081203A 93 s after the trigger beginning with a 150 s *white*-filter finding chart, followed by a 50 s UV-grism exposure starting 251 s after the trigger, a second finding chart in *u* and then exposures in the other UVOT photometric filters (De Pasquale & Parsons 2008). The UV-grism spectrum was taken during the decay of the second BAT gamma-ray peak. The best source position was determined by the UVOT, which located a fading source at $RA_{J2000} = 15^{\text{h}}32^{\text{m}}07^{\text{s}}.58 (=233^{\circ}.03158)$ $Dec_{J2000} = +63^{\text{d}}31^{\text{m}}14^{\text{s}}.9 (=63^{\circ}.52081)$, with an uncertainty of 0.5 arcsec (90 per cent confidence limit; De Pasquale & Parsons 2008), consistent with the refined XRT position (Goat et al. 2008). Using the grism spectrum, a provisional redshift of 2.1 was reported by Landsman et al. (2008). The X-ray spectrum, extracted from the XRT Window Timing data, overlaps with the grism exposure and has an exposure time of 558 s, starting 87 s after the trigger (La Parola et al. 2008).

The source was detected in the *u*, *b*, *v*, *white*, *uvw1* filters, and only faintly in the *uvw2* filter. It was not detected in the *uvm2* filter, which is consistent with the filter response curves and the shape of the UV-grism spectrum. The brightness of the GRB can be measured from the zeroth order of the grism image, which provides a magnitude of $b = 13.76 \pm 0.23$ at the time of the grism exposure. Folding the extracted spectrum (see Section 3) through the *u*-filter response leads to a magnitude of 13.4 during the grism exposure with a systematic error estimated to be 25 per cent. The light curve of GRB 081203A is shown in Fig. 1.

A cutout of the grism image with the GRB spectrum is shown in Fig. 2. The zeroth order of a 15th magnitude star falls on the GRB spectrum around 5000 \AA . The image was processed using the HEADAS-6.5.1 software to remove the MODULO-8 pattern (Poole et al. 2008).

The raw count rate spectrum was extracted using the UVOTIMGRISM program. The data were binned up by a factor of 3, which reduces any correlation caused by the image rotation during the spectral

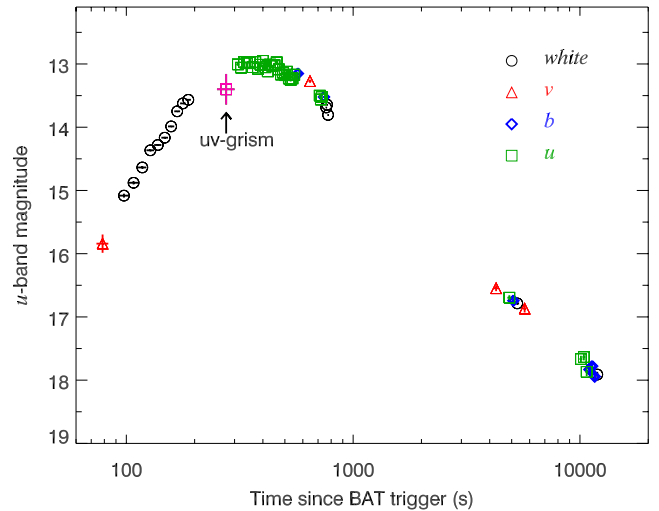


Figure 1. The light curve of GRB 081203A shows that the spectrum was taken during the rise. The photometry point derived from the spectrum, indicated with an arrow, has a larger uncertainty than those of the lenticular filters.

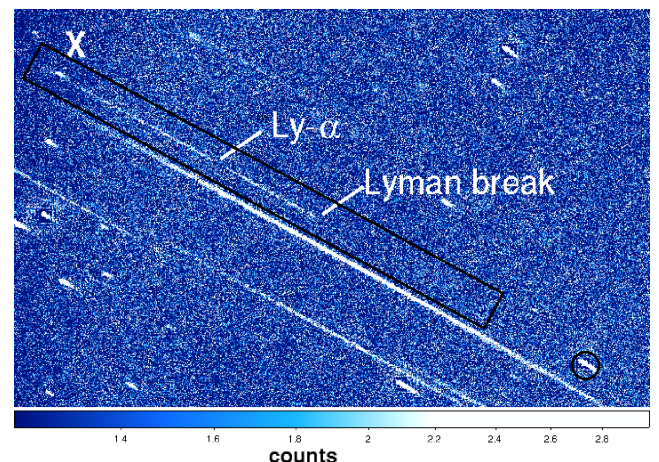


Figure 2. The UV-grism image of GRB 081203A. The GRB first-order spectrum is inside the black rectangle. The zeroth order is indicated by a black circle. The ‘X’ in the top-left corner indicates the contaminating zeroth order of a star.

extraction but keeps the bin size smaller than the wavelength resolution. The wavelength scale was adjusted to the latest UV-grism wavelength calibration (to be released shortly) for the nominal filter wheel position, and is accurate to 15 \AA . The UV-grism spectrum has a resolution of $R \approx 150$ at 2600 \AA , with a dispersion of $\sim 3.2 \text{ \AA pixel}^{-1}$. It can be seen that bluewards of 2780 \AA no signal above the background is seen. Although wavelengths in the first-order spectrum longer than 2850 \AA can be contaminated by a second-order spectra, this is not a concern here since there is no source flux shortwards of 2780 \AA , thus, the second-order spectrum will only affect the first order for wavelengths longer than 5549 \AA .

3 SPECTRAL MODELLING

The background-subtracted spectrum of GRB 081203A is provided in Fig. 3, overlaid by our best-fitting spectral model. Calibrations for the wavelength scale, line spread function and

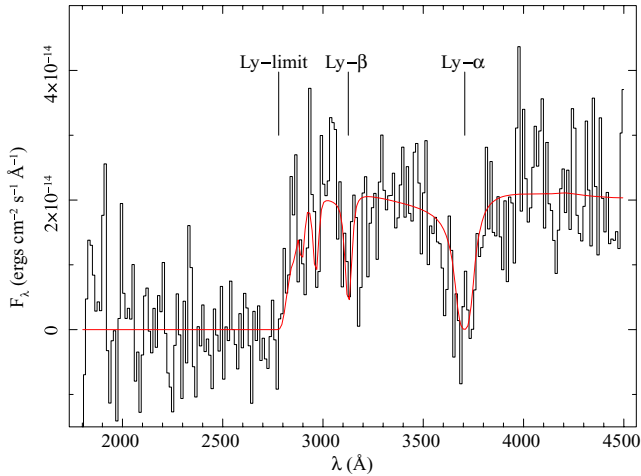


Figure 3. The UV-grism first-order spectrum of GRB 081203A. The model shown here as a red line includes the Lyman forest as discussed in Section 3.

telescope throughput have been extracted from a development version of the *Swift* calibration data base. Wavelengths are currently good to 0.5 per cent systematic accuracy (1σ) and the flux calibration is good to an estimate of 25 per cent.

Neglecting the systematic uncertainty in the wavelength scale, Fig. 3 reveals a broad absorption line at $3706 \pm 11 \text{ \AA}$ that we identify with the $\text{Ly}\alpha$ transition of hydrogen, and a corresponding Lyman continuum edge at $2779 \pm 8 \text{ \AA}$, shortwards of which no significant source detection is made. $\text{Ly}\beta$ is weakly detected at $3126 \pm 8 \text{ \AA}$. Wavelength errors and the best-fitting parameters are at the 1σ level.

Within the spectral model, the afterglow continuum is characterized by a single power law attenuated by neutral gas and dust from both the Milky Way and host galaxy of the burst. Both galactic and host galaxy continuum absorption at wavelengths shorter than the Lyman edge are modelled using the photoelectric cross-sections of Morrison & McCammon (1983) and the relative element abundances of Anders & Ebihara (1982). The Milky Way extinction law has been taken from the analytical description of Pei (1992), and the host extinction is assumed to be identical to the Small Magellanic Cloud law also from Pei (1992). Host galaxy hydrogen Lyman series absorption from $n = 1\text{--}100$ is modelled following the algorithm described in Totani et al. (2006) and based upon Peebles (1991). Oscillator strengths for transitions $n = 1\text{--}31$ are taken from Morton (1991) and extrapolated to $n \leq 100$ thereafter. The wavelength-dependent optical depth calculated within the model is also broadened by a macroscopic velocity field within the absorbing column. We assume a Gaussian velocity field, characterized by its full-width half-maximum (FWHM) velocity.

The combined model contains four free parameters: cosmological redshift (z), neutral hydrogen column density ($N_{\text{H,I}}$), FWHM of the absorbers velocity field (v) and the normalization of the afterglow continuum. In order to constrain the continuum emission over the relatively narrow spectral range of the UV-grism, five additional model parameters are pre-determined. The Galactic column density towards the burst, $\log N_{\text{H,g}} = 20.23$, is taken from the map of Kalberla et al. (2005). Galactic dust is quantified by the extinction coefficient $A_{\text{V,g}} = 0.06$, taken from Schlegel, Finkbeiner & Davis (1998). The continuum spectral index ($\beta = 0.90 \pm 0.01$), the neutral column density within the host galaxy ($\log N_{\text{H,h}} = 21.7 \pm 0.1$) and the host galaxy dust extinction coefficient ($A_{\text{V,h}} = 0.08$) were

all measured by a fit to the broad-band spectral energy distribution (SED) of the afterglow, interpolated to the $T+700$ s epoch and incorporating six lenticular filter magnitudes from the UVOT and the X-ray spectrum from the XRT. This method is described by Schady et al. (2007). The detailed fit to the SED will be provided in a forthcoming paper concerning the spectral and temporal behaviour of GRB 081203A.

The model fit to the grism spectrum was performed using XSPEC 12.5.0 (Arnaud 1996). The best fit provides $\chi^2 = 301.9$ for 231 degrees of freedom (d.o.f.), $\log N_{\text{H,I}} = 22.09^{+0.09}_{-0.12}$, $z = 2.046 \pm 0.002$ and $v < 598 \text{ km s}^{-1}$ (90 per cent confidence limit). The significance of the line detections was determined by freezing the redshift. The fit to the spectrum in the 3400–4000 \AA wavelength range gives a 4.0σ detection of $\text{Ly}\alpha$, and $\text{Ly}\beta$ is detected at the 1.5σ level in the 3000–3300 \AA wavelength range. The best-fitting column density satisfies the definition for a damped $\text{Ly}\alpha$ absorption system (DLA). Taking into account systematic errors in the wavelength dispersion, $z = 2.05 \pm 0.01$.

At a redshift of 2.05, we expect some contamination in the spectrum from absorption systems located between the Earth and the host (Madau 1995). Within the limits of the signal-to-noise ratio, there is no compelling evidence for discrete $\text{Ly}\alpha$ absorption from intervening galaxies. We do however investigate whether an undetected, or unresolved, Lyman forest could have an impact on the measured properties. We add the statistically based algorithm characterizing the cosmological hydrogen density from Madau (1995) to the model, which effectively absorbs photons bluewards of the host galaxy $\text{Ly}\alpha$ line (Fig. 3). The best fit for this situation provides $\chi^2 = 271.4$ for 231 d.o.f., $\log N_{\text{H,I}} = 22.02^{+0.11}_{-0.12}$, $z = 2.05 \pm 0.01$ and $v < 474 \text{ km s}^{-1}$. The Madau model gives a slightly better fit to the data.

4 DISCUSSION AND CONCLUSIONS

With the rapid and precise locations of GRBs available with *Swift*, the number of GRBs available with good signal-to-noise ratio spectroscopic data has doubled. Of these, 16 per cent have an associated DLA (Jakobsson et al. 2006; Prochaska et al. 2007). The column density of $N_{\text{H,I}} = 1.04 \times 10^{22} \text{ cm}^{-2}$ in GRB 081203A is typical of GRB DLAs (Prochaska et al. 2008), but its redshift is amongst the smallest of the sample (see Fig. 4). It also has the lowest redshifts observed in a GRB for which both the Lyman break and $\text{Ly}\alpha$ have been obtained.

Since it is possible for UVOT spectra to be taken during the rising phase of the afterglow, and while the gamma-ray emission is still in progress, as was the case for GRB 081203A, useful constraints on the evolution of the ionization state of the gas in the GRB environment may be obtained by comparison to ground-based spectra taken later in the decay phase of the afterglow. Getting an early spectrum with UVOT opens up the opportunity to increase the sample of *Swift* GRBs with redshifts. As well as its obvious advantage for UV coverage, the UVOT is capable of taking spectra of GRBs with positions that are unobtainable for ground-based observations. Indeed, GRB 081203A was a twilight object for ground-based observers, and we are not aware of any ground-based spectroscopic follow-up of this object.

We have shown that it is possible to obtain useful spectra using the UVOT UV-grism in the automated *Swift* response to new GRBs. The combined measurement of the Ly continuum edge, $\text{Ly}\alpha$ and possibly $\text{Ly}\beta$ provides a good measurement of the redshift in the UVOT UV-grism spectra for redshifts of GRBs between $0.5 < z < 3.5$. Using such spectra, we expect to find new DLAs in the range

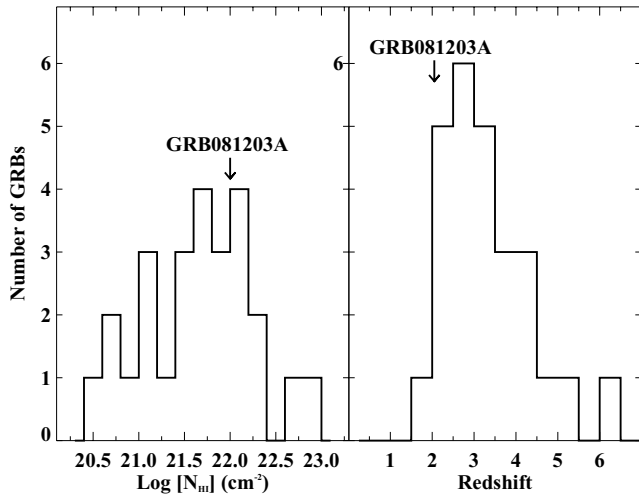


Figure 4. The figure shows the number of GRBs with an associated DLA. The left-hand panel shows that the $N_{\text{H I}}$ column density of GRB 081203A as determined in this Letter is quite typical. The right-hand panel shows that the redshift of GRB 081203A is one of the lowest measured for a GRB with a DLA. The UVOT is capable of measuring redshifts below $z = 1.9$ that cannot be measured from the ground. The data for this figure were taken from the literature (Jakobsson et al. 2006; Prochaska et al. 2007; Savaglio, private communication).

$0.5 < z < 2.0$. *Swift* observations can, in principle, probe the different components of the interstellar medium by providing a measurement of H I from the grism spectrum, dust extinction from the photometry and metallicity from the X-rays.

ACKNOWLEDGMENTS

This work was supported by the UK Science and Technology Facilities Council through a grant for *Swift* Post Launch Support at UCL-MSSL. This work is sponsored at PSU by NASA contract NAS5-00136. We acknowledge useful comments by the anonymous referee which led to improvement of the grism analysis. We would like to dedicate this Letter to the late Richard Bingham, whose visionary optical design for the UVOT grism made these observations possible.

REFERENCES

- Anders E., Ebihara M., 1982, *Geochim. Cosmochim. Acta*, 46, 2363
 Arnaud K. A., 1996, in Jacoby G., Barnes J., eds, *ASP Conf. Ser. Vol. 101, Astronomical Data Analysis Software and Systems V*. Astron. Soc. Pac., San Francisco, p. 17
 Barthelmy S. et al., 2005, *Space Sci. Rev.*, 120, 143
 Burrows D. et al., 2005, *Space Sci. Rev.*, 120, 165
 De Pasquale M., Parsons A., 2008, *GCN Circ. No. 8603*
 Gehrels N. et al., 2004, *ApJ*, 611, 1005
 Goad M., Osborne J. P., Beardmore A. P., Evans P. A., 2008, *GCN Circ. No. 8598*
 Jakobsson P., Kalberla P. M. W., Burton W. B., Hartmann D., Arnal E. M., Bajaja E., Morris R., Pöppel W. G. L., 2006, *A&A*, 460, L13
 Kalberla P. M. W. et al., 2005, *A&A*, 440, 775
 Landsman W. B., De Pasquale M., Kuin N. P. M., Schady P., Smith P., Parsons A., 2008, *GCN Circ. No. 8601*
 La Parola V., Sbarufatti B., Mangano V., Parsons A., 2008, *GCN Circ. No. 8609*
 Madau P., 1995, *ApJ*, 441, 18
 Morrison R., McCammon D., 1983, *ApJ*, 270, 119
 Morton D. C., 1991, *ApJS*, 77, 119
 Parsons A. et al., 2008, *GCN Circ. No. 8595*
 Peebles P. J. E., 1993, *Principles of Physical Cosmology*. Princeton Univ. Press, Princeton, NJ
 Pei Y. C., 1992, *ApJ*, 395, 130
 Poole T. et al., 2008, *MNRAS*, 383, 627
 Prochaska J. X., Chen H.-W., Wolfe A. M., Dessauges-Zavadsky M., Bloom J. S., 2007, *ApJ*, 666, 267
 Prochaska J. X., Dessauges-Zavadsky M., Ramirez-Ruiz E., Chen H.-W., 2008, *ApJ*, 685, 344
 Roming P. W. A. et al., 2005, *Space Sci. Rev.*, 120, 95
 Roming P. W. A. et al., 2006, *ApJ*, 652, 1416
 Roming P. W. A. et al., 2009, *ApJ*, 690, 163
 Schady P. et al., 2007, *MNRAS*, 377, 273
 Schlegel D. J., Finkbeiner D. P., Davis M., 1998, *ApJ*, 500, 525
 Smette A. et al., 2001, *ApJ*, 556, 70
 Totani T., Kawai N., Kosugi G., Aoki K., Yamada T., Iye M., Ohta K., Hatterri T., 2006, *PASJ*, 58, 485

This paper has been typeset from a $\text{\TeX}/\text{\LaTeX}$ file prepared by the author.